Eur. J. Mech. B - Fluids 19 (2000) 491–502

S0997-7546(00)00135-7/FLA

Merging and wetting driven by surface tension

Joseph B. Keller [a,1], Paul A. Milewski [b,2], Jean-Marc Vanden-Broeck [b,3]

[a] *Departments of Mathematics and Mechanical Engineering, Stanford University, Stanford, CA 94305–2125, USA*
[b] *Department of Mathematics, University of Wisconsin–Madison, Madison, USA*

(Received 22 November 1999; revised and accepted 22 March 2000)

Abstract – The surface tension driven merging of two wedge-shaped regions of fluid, and the wetting of a wedge shaped solid, are analyzed. Following the work of Keller and Miksis in 1983, initial conditions are chosen so that the flows and their free surfaces are self-similar at all times after the initial contact. Then the configuration magnifies by the factor $t^{2/3}$ and the fluid velocity at the point $\mathbf{x}/t^{2/3}$ decays like $t^{-1/3}$, where the origin of $\mathbf{x}$ and t are the point and time of contact. In the merging problem the vertices of the two wedges of fluid are initially in contact. In the wetting problem, the vertex of a wedge of fluid is initially at the corner of the solid. The motions and free surfaces are found numerically. These results complement those of Keller and Miksis for the wetting of a single flat surface and for the rebound of a wedge of fluid after it pinches off from another body of fluid. © 2000 Éditions scientifiques et médicales Elsevier SAS

wetting / merging / necking / surface tension / self-similar

1. Introduction

The merging of two bodies of liquid and the wetting of a solid by a liquid both involve the rapid transient motion of a liquid with a free surface at which surface tension acts. Some aspects of such motions are elucidated by the self-similar flows introduced by Keller and Miksis [1]. Self-similar flows are quite special, but they are sometimes attractors which are approached by certain other flows as they evolve. Therefore, we shall investigate some self-similar merging and wetting flows.

We consider the wetting of a solid by a fluid which comes in contact with it at the corner $\mathbf{x} = 0$ at $t = 0$ (see *figure 1(a)*), and the merging of two regions of fluid which meet at one point $\mathbf{x} = 0$ at time $t = 0$ (see *figure 1(b)*). In both cases, the motion is driven by surface tension, and is singular at $t = 0$. The fluid is surrounded by a gas at constant pressure.

To analyze these phenomena, we take the fluid to be incompressible, inviscid, and in irrotational motion in two dimensions. Following Keller and Miksis [1] we assume that the initial configuration contains no length scale. This is the case if the fluid is initially at rest and if the solid and fluid surfaces at $t = 0$ are straight lines meeting at the point $\mathbf{x} = 0$. (See *figures 1(a)* and *1(b)*.) Then it follows that in the merging problem, the velocity and surface of the fluid are self-similar at all later times. The velocity is of the form $(\sigma/\rho t)^{1/3}\,\mathbf{u}[(\rho/\sigma t^2)^{1/3}\mathbf{x}]$ and the equation of the free surface is of the form $f[(\rho/\sigma t^2)^{1/3}\mathbf{x}] = 0$, where ρ is the fluid density and σ is the coefficient of surface tension. Thus the configuration just magnifies by the factor $t^{2/3}$ and the velocity at $\mathbf{x}/t^{2/3}$ decays like $t^{-1/3}$.

[1] Correspondence and reprints; e-mail: keller@math.stanford.edu
[2] E-mail: milewski@math.wisc.edu
[3] Present address: School of Mathematics, University of East Anglia, Norwich, UK; e-mail: J.Vanden-broeck@uea.ac.uk

In the wetting problem, the same self-similarity will result if the contact angle β is a constant, independent of the velocity of the contact line. However, both experiment and theory show that β varies with the velocity of the contact line when that velocity is small. But when the velocity is large, as it is initially in wetting, β seems to be constant. Therefore, to describe the initial behavior of the wetting flow, we shall take β to be constant. Some of the previous work on the velocity dependence of β is described in section 5.

In section 2 we give a detailed formulation of the wetting problem, including the requirement of a fixed contact angle β between the fluid and solid surfaces. We treat only flows symmetric about the y-axis. The fluid is bounded initially by the semi-infinite straight lines with slope angles θ and $\pi - \theta$, so it occupies a wedge of opening angle $\pi - 2\theta$. The merging problem shown in *figure 1(b)* is a special case of the wetting problem shown in *figure 1(a)*, in which $\beta = \pi/2$ and $\alpha = 0$, i.e. the free surface is normal to the wall and the wall is flat. The case of wetting when $\alpha < 0$ and $\theta = 0$ is particularly interesting since it corresponds to the wetting of a solid wedge whose tip touches a flat fluid surface at $t = 0$. A typical configuration is shown in *figure 1(c)* which was turned upside down.

In section 3 we reformulate the problem as an integro-differential system. In section 4 we present a numerical method for solving this system and discuss the results. Some of them are shown in *figures 2* to *6*. In section 5 we discuss the results and their applicability.

2. Formulation

We consider a rigid boundary consisting of two semi-infinite straight walls $A'O$ and $C'O$ which meet at the corner O. (See *figure 1(a)*.) Between the walls is a wedge-shaped region of fluid bounded by two semi-infinite straight lines BO and DO. The line $C'O$ makes the angle α with the positive x-axis, and $A'O$ makes the same angle with the negative x-axis, so that the angle between the walls is $\pi - 2\alpha$. The line DO makes the angle $\theta > \alpha$ with the positive x-axis, and BO makes the same angle with the negative x-axis, so the fluid occupies the angle $\pi - 2\theta$.

At $t = 0$ the fluid begins to move under the influence of surface tension, wetting the walls along the segments OA and OC, and making the contact angle β with each wall. The two free surfaces of the fluid are deformed into the two curved lines AB and CD. Since the initial configuration is symmetric about the y-axis, the resulting flow will be symmetric also. Therefore we shall formulate the problem for that half of the flow in the region $x > 0$.

The symmetrical merging of two identical wedges of fluid is represented in *figure 1(b)*. By comparing this figure with *figure 1(a)* we see that the upper half of the merging flow is the same as the wetting flow when the corner is absent, i.e. when $\alpha = 0$, and the wetting angle is $\beta = \pi/2$. Therefore we shall just formulate and solve the wetting problem, and obtain the merging flow by setting $\alpha = 0$ and $\beta = \pi/2$.

The fluid velocity can be written as $\nabla\Phi(\mathbf{x}, t)$ where the potential Φ is a harmonic function in the fluid domain $\Omega(t)$:

$$\Delta\Phi = 0, \quad \mathbf{x} \in \Omega(t). \tag{1}$$

The free boundary CD of $\Omega(t)$, is described by $F(\mathbf{x}, t) = 0$. On this boundary, the kinematic and dynamic boundary conditions are, respectively,

$$F_t + \nabla\Phi \cdot \nabla F = 0 \quad \text{on } F = 0, \tag{2}$$

$$\Phi_t + \frac{1}{2}(\nabla\Phi)^2 + (\sigma/\rho)\kappa = 0 \quad \text{on } F = 0. \tag{3}$$

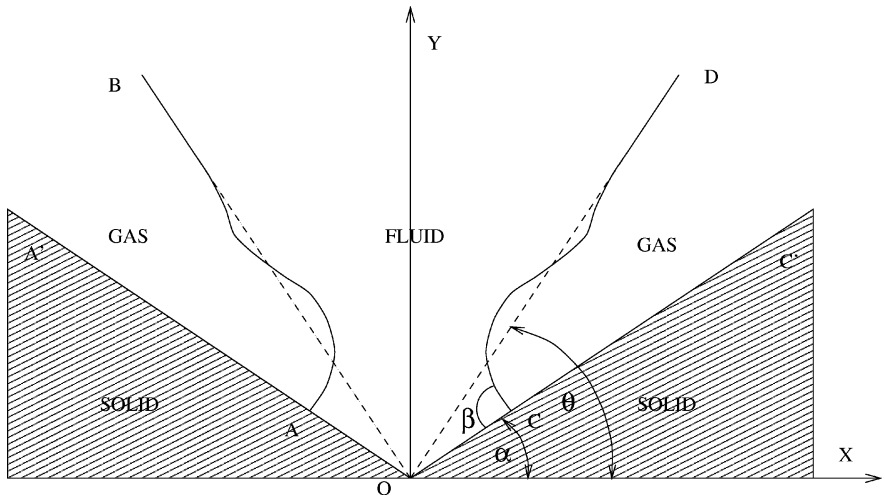

(a)

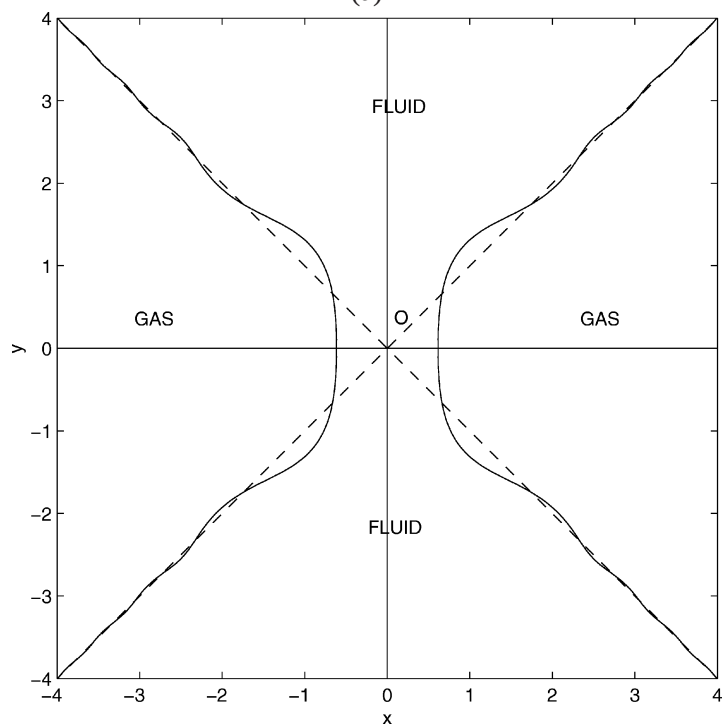

(b)

Figure 1. (a) A fluid wetting the walls near a corner. One solid wall OC, makes the angle α with the positive x-axis and the other solid wall, OA, makes the same angle with the negative x-axis. The fluid is contained initially (at $t = 0$) in the wedge bounded by the dotted lines OD and OB, which make the angle θ with the positive and negative x-axes, respectively. For $t > 0$, the free surfaces of the fluid are the curved lines CD and AB, which meet the solid walls at the contact angle β. The segments OC and OA of the walls are wetted. (b) Typical result of the merging of two wedges of fluid. For $t > 0$, the free surface in the first quadrant was computed by the method of section 3 with $\alpha = 0°$, $\theta = 45°$, and $\beta = 90°$. (c) Typical result of the wetting of a solid wedge by an initially horizontal fluid region. For $t > 0$, the free surface for $\xi > 0$ was computed by the method of section 3 with $\alpha = -40°$, $\theta = 0°$, and $\beta = 90°$. The figure has been turned upside down.

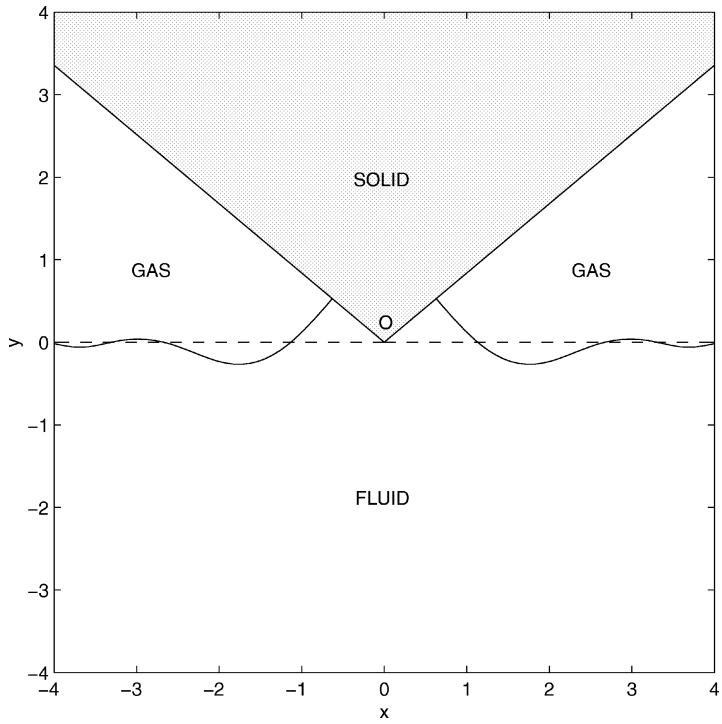

(c)

Figure 1. (Continued.)

Here, σ is the coefficient of surface tension, ρ is the density of the fluid, and κ is the curvature of the free surface. The symmetry about the y-axis implies

$$\Phi_x = 0 \quad \text{on } x = 0. \tag{4}$$

The kinematic condition on OC is

$$\Phi_x \sin\alpha - \Phi_y \cos\alpha = 0 \quad \text{on } OC. \tag{5}$$

The contact angle condition at C implies

$$F_x \cos(\alpha - \beta) + F_y \sin(\alpha - \beta) = 0 \quad \text{at } C. \tag{6}$$

To fix the velocity potential uniquely, we assume that

$$\Phi \to 0 \quad \text{as } x^2 + y^2 \to \infty. \tag{7}$$

Initially, at $t = 0$, we require that

$$\Phi(\mathbf{x}, 0) = 0, \tag{8}$$

$$F(\mathbf{x}, 0) = y\cos\theta - x\sin\theta. \tag{9}$$

This concludes the formulation of the problem. For given values of α, β and θ, we seek Φ and the curve $F = 0$ such that (1)–(9) are satisfied.

Since this problem contains no length scale, we shall seek a solution expressed in terms of the dimensionless similarity variables ξ and η defined by

$$\xi = x\left(\rho/\sigma t^2\right)^{1/3}, \qquad \eta = y\left(\rho/\sigma t^2\right)^{1/3}. \tag{10}$$

We write Φ and F in terms of two new functions φ and f:

$$\Phi(x, y, t) = \left(\sigma^2 t/\rho^2\right)^{1/3}\varphi(\xi, \eta), \tag{11}$$

$$F(x, y, t) = f(\xi, \eta). \tag{12}$$

The domain $\Omega(t)$ becomes a fixed domain Ω_0 in the ξ, η variables, with the equation of the free boundary given by $f(\xi, \eta) = 0$. Substituting (10)–(12) into (1)–(3) yields,

$$\Delta\varphi = 0 \quad \text{in } \Omega_0, \tag{13}$$

$$-\frac{2}{3}(\xi, \eta)\cdot\hat{n} + \nabla\varphi\cdot\hat{n} = 0 \quad \text{on } f = 0, \tag{14}$$

$$-\frac{2}{3}(\xi, \eta)\cdot\nabla\varphi + \frac{1}{2}(\nabla\varphi)^2 + \frac{1}{3}\varphi + \kappa = 0 \quad \text{on } f = 0. \tag{15}$$

In (14), $\hat{n}$ denotes the unit normal pointing out of Ω_0. Equations (4)–(7) remain unchanged with Φ, x, y, F replaced by φ, ξ, η, f respectively. Equation (8) follows from (11) if φ is bounded at infinity, while (9) and (12) yield

$$f(\xi, \eta) \sim \eta\cos\theta - \xi\sin\theta \quad \text{as } \xi^2 + \eta^2 \to \infty. \tag{16}$$

3. Reformulation as an integro-differential system

To solve the problem formulated above, we first express the free surface $f(\xi, \eta) = 0$ parametrically in terms of arclength s along it, with $s = 0$ at C: $\xi = \bar{\xi}(s),\ \eta = \bar{\eta}(s)$. Then

$$\bar{\xi}'^2 + \bar{\eta}'^2 = 1. \tag{17}$$

The tangent $\hat{t}$ and the normal $\hat{n}$ are given by

$$\hat{t} = (\bar{\xi}', \bar{\eta}'), \qquad \hat{n} = (\bar{\eta}', -\bar{\xi}'), \tag{18}$$

and the curvature κ is

$$\kappa = \bar{\xi}'\bar{\eta}'' - \bar{\eta}'\bar{\xi}''. \tag{19}$$

On the boundary the gradient of φ can be written as

$$\nabla\varphi = \hat{n}\frac{\partial\varphi}{\partial n} + \hat{t}\frac{\partial\varphi}{\partial s}. \tag{20}$$

By using these relations, we can write the boundary conditions (14) and (15) as

$$\frac{\partial\varphi}{\partial n} = \frac{2}{3}(\bar{\xi}\bar{\eta}' - \bar{\eta}\bar{\xi}'), \tag{21}$$

$$-\frac{2}{3}(\bar{\xi}\bar{\xi}' + \bar{\eta}\bar{\eta}')\frac{\partial\varphi}{\partial s} + \frac{1}{2}\left(\frac{\partial\varphi}{\partial s}\right)^2 - \frac{1}{2}\left(\frac{\partial\varphi}{\partial n}\right)^2 + \frac{1}{3}\varphi + \bar{\xi}'\bar{\eta}'' - \bar{\eta}'\bar{\xi}'' = 0. \tag{22}$$

The contact angle condition (6) becomes

$$\bar{\eta}'\cos(\alpha-\beta) - \bar{\xi}'\sin(\alpha-\beta) = 0 \quad \text{at } s = 0. \tag{23}$$

On the free surface, the far field conditions (7) and (16) become, respectively,

$$\varphi \sim 0 \quad \text{as } s \to \infty, \tag{24}$$

$$\bar{\eta}\cos\theta - \bar{\xi}\sin\theta \sim 0 \quad \text{as } s \to \infty. \tag{25}$$

We introduce the Green's function $G(\xi, \eta, \xi^*, \eta^*)$ with the slowest growth at infinity satisfying

$$\Delta G = \delta(\xi - \xi^*, \eta - \eta^*), \tag{26}$$

$$\frac{\partial G}{\partial\xi} = 0 \quad \text{on } \xi = 0, \tag{27}$$

$$\sin\alpha\frac{\partial G}{\partial\xi} - \cos\alpha\frac{\partial G}{\partial\eta} = 0 \quad \text{on } \eta\cos\alpha - \xi\sin\alpha = 0. \tag{28}$$

For $\alpha = 0$ the Green's function is given by

$$\begin{aligned} G = {} & \frac{1}{2\pi}\ln\left[(\xi-\xi^*)^2 + (\eta-\eta^*)^2\right]^{1/2} + \frac{1}{2\pi}\ln\left[(\xi-\xi^*)^2 + (\eta+\eta^*)^2\right]^{1/2} \\ & + \frac{1}{2\pi}\ln\left[(\xi+\xi^*)^2 + (\eta-\eta^*)^2\right]^{1/2} + \frac{1}{2\pi}\ln\left[(\xi+\xi^*)^2 + (\eta+\eta^*)^2\right]^{1/2}. \end{aligned} \tag{29}$$

For other values of α we can obtain G from this formula by conformal mapping.

We now apply Green's theorem in Ω_0 to φ and G, writing $G(s, s^*) = G[\bar{\xi}(s), \bar{\eta}(s), \bar{\xi}(s^*), \bar{\eta}(s^*)]$ and $\varphi(s) = \varphi[\bar{\xi}(s), \bar{\eta}(s)]$. The only nonzero contribution to the integrals comes from the free surface, so we get

$$\frac{1}{2}\varphi(s^*) = \int_0^\infty \left[\varphi(s)\frac{\partial G}{\partial n}(s, s^*) - G(s, s^*)\frac{\partial\varphi}{\partial n}(s)\right] \mathrm{d}s. \tag{30}$$

Equation (30), together with the conditions (17) and (21)–(25) define an integro-differential system for the unknowns $\bar{\xi}(s)$, $\bar{\eta}(s)$, $\varphi(s)$.

4. Numerical method

The integro-differential system derived in section 3 can be solved numerically. To solve it we discretize a portion of the free surface with $N+1$ equally spaced points s_i, $i = 0, \ldots, N$, with $s_0 = 0$. The corresponding

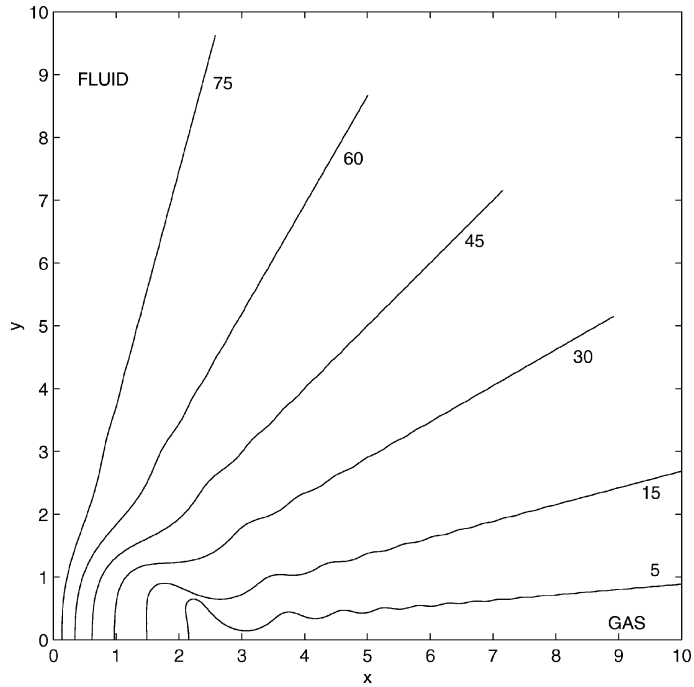

Figure 2. Six cases of merging of two wedges of fluid. That part of the computed free surface of the upper wedge which lies in the first quadrant is shown for $t > 0$. In all cases $\alpha = 0°$ and $\beta = 90°$. The values of θ, from bottom to top, are $\theta = 5°, 15°, 30°, 45°, 60°, 75°$. In the first two cases, the computational domain exceeded the region shown. Reflection in the x and y axes will yield the full picture of the merged fluids, as in *figure 1(b)*.

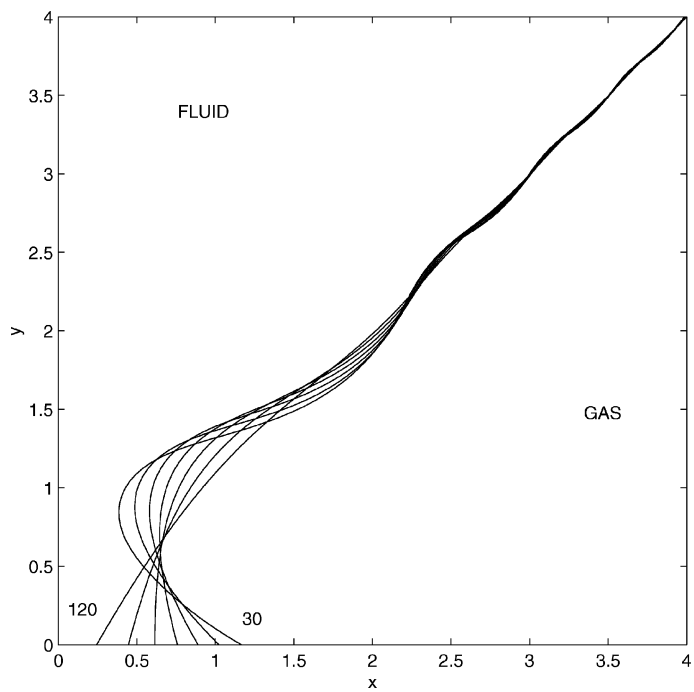

Figure 3. Six cases of a wedge of fluid wetting a plane. The flow is symmetric about the y-axis At $t = 0$ the fluid in $x > 0$ is bounded by the line $\theta = 45°$. The solid plane is the x-axis, so $\alpha = 0°$. The values of the contact angle β are, from left to right, $\beta = 120°, 105°, 90°, 75°, 60°, 45°, 30°$. Only part of each computational domain is shown.

$3N+3$ unknowns are φ_i, ξ_i, η_i. We compute all derivatives at interior points with centered finite difference stencils. The arclength equation (17) is satisfied at the midpoints $s_i^M = (s_i + s_{i+1})/2$ for $i = 0, \ldots, N-1$. Bernoulli's equation (22) is satisfied at s_i, for $i = 1, \ldots, N$. The integral equation (30) is applied at s_i^M for $i = 1, \ldots, N-2$ with the trapezoidal rule for the integral, summing over s_j where $j = 0, \ldots, N$. This approximates correctly the principal value integral in (30). Together these yield $3N-2$ nonlinear algebraic equations for the $3N+3$ unknowns φ_i, ξ_i and η_i, $i = 0, \ldots, N$. Three more equations come from the conditions (23) at s_0 and (24) and (25) at s_N. One more equation forces the first free surface point (ξ_0, η_0) to be on the wall

$$\bar{\xi}(0)\sin\alpha - \bar{\eta}(0)\cos\alpha = 0. \tag{31}$$

The final equation is obtained by combining (21) with (5):

$$\sin\beta\frac{\partial\varphi}{\partial s}(0) = -\frac{2}{3}\cos\beta\left[\bar{\xi}(0)\bar{\eta}'(0) - \bar{\eta}(0)\bar{\xi}'(0)\right]. \tag{32}$$

The resulting system of $3N+3$ equations for $3N+3$ unknowns is solved by Newton's method using continuation. We start from the exact solution $\varphi = 0$, $\xi = s\cos\theta$, $\eta = s\sin\theta$, which holds when $\beta + \theta - \alpha = \pi$. Then we gradually change θ, α or β keeping $\beta < \pi - \theta + \alpha$.

We have used this scheme to compute solutions for various values of θ, α, β. Some of the results are shown in *figures 1(b), 1(c), 2, 3, 4,* and *5*. The numerical results shown have converged, since varying N and Δs does not change them. Typical calculations involve $N = 200$, $\Delta s = 0.05$.

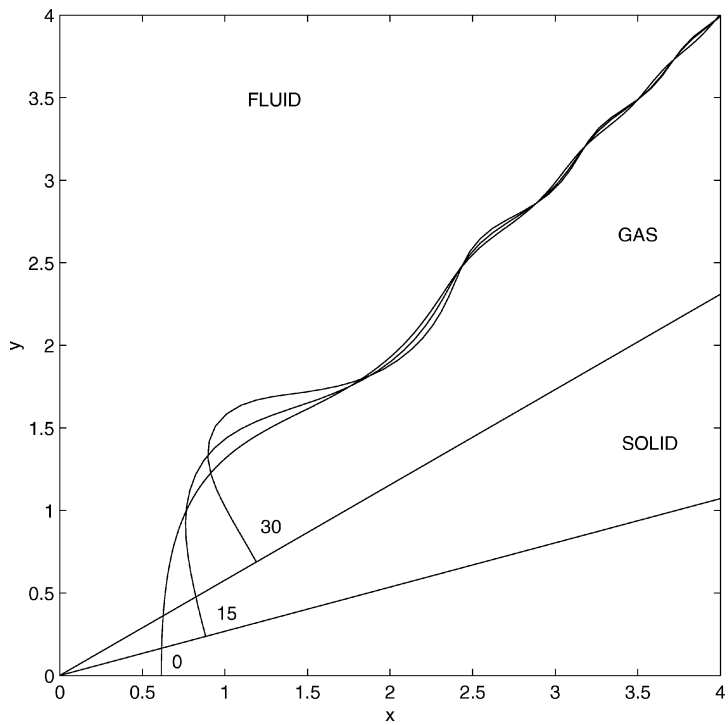

Figure 4. Three cases of a wedge of fluid wetting a solid near a corner. The configuration is symmetric in the y-axis, so the other wall of the corner is in the second quadrant. In each case the initial boundary of the liquid is the line $\theta = 45°$, and the contact angle is $\beta = 90°$. The values of α shown on the figure are $\alpha = 0°, 15°, 30°$. Only part of each computational domain is shown.

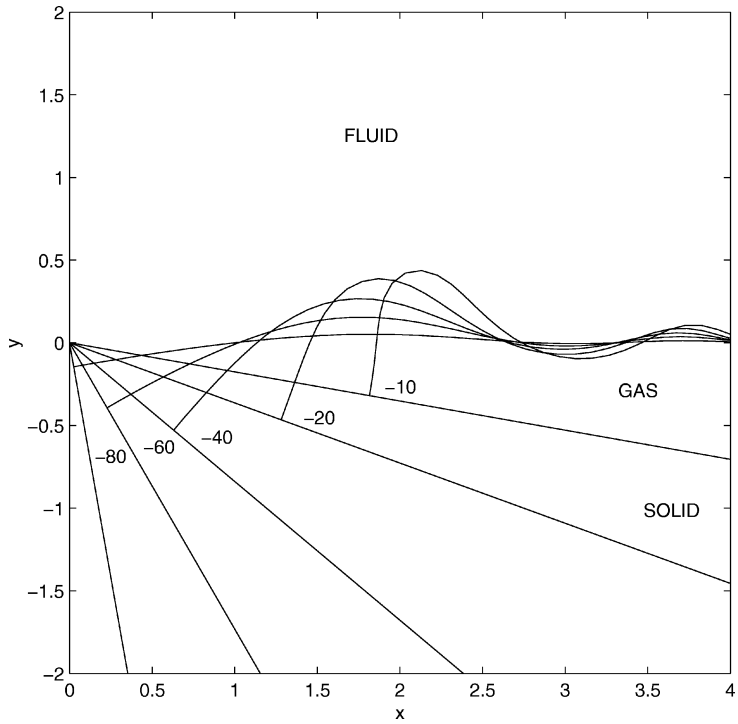

Figure 5. Five cases of a solid wedge being wet by a half-plane of fluid. The configuration is symmetric in the y-axis, so the other wall of the corner is in the third quadrant. The boundary of the liquid is initially horizontal and the wedge touches the fluid at $t = 0$. The contact angle $\beta = 90°$, and $\alpha = -10°, -20°, -40°, -60°, -80°$, corresponding to wedges of $160°, 140°, 100°, 60°, 20°$ respectively. Only part of the computational domain is shown.

5. Discussion of results

Figure 2 shows the results for merging of two fluid wedges with various values of θ. They were computed with $\alpha = 0$ and $\beta = \pi/2$, and must be reflected in the two axes to show the entire flow, as was done in *figure 1(b)* for the case $\theta = 45°$.

From *figure 2* we see that the width of the neck between the two bodies of fluid is greater the smaller the angle 2θ between their surfaces. This is shown graphically in *figure 6(a)*, where the half-width of the neck is plotted as a function of θ. The width appears to tend to infinity as θ tends to zero, indicating that a much more rapid merging will occur initially for two liquid bodies, such as drops, with smooth surfaces which are tangent to one another. It would be worthwhile to determine analytically the nature of the singular behavior of the width near $\theta = 0$ shown in *figure 6(a)*, and also that in *figure 6(c)* which will be described below.

Figure 2 also shows waves on the surface of the fluid. These are capillary waves generated by the motion of each fluid in response to the impulsive force exerted by the other fluid. Their amplitude increases as θ decreases. These waves also appear when a column of fluid pinches off and the two portions are pulled apart by surface tension. In that context, they have been examined by Keller and Miksis [1], and in the far field they were shown to have the form of capillary waves impulsively generated at a point. They were also treated in the linear analysis of pinch-off by Lawrie [2] and Lawrie and King [3], and in the slender wedge analysis of pinch-off by Ting and Keller [4] and King [5]. The problem treated in [1] was generalized to the case of two fluids by Popple, Billingham, and King [6]. The merging of two wedges of viscous fluid was analyzed by Miksis and Vanden-Broeck [7].

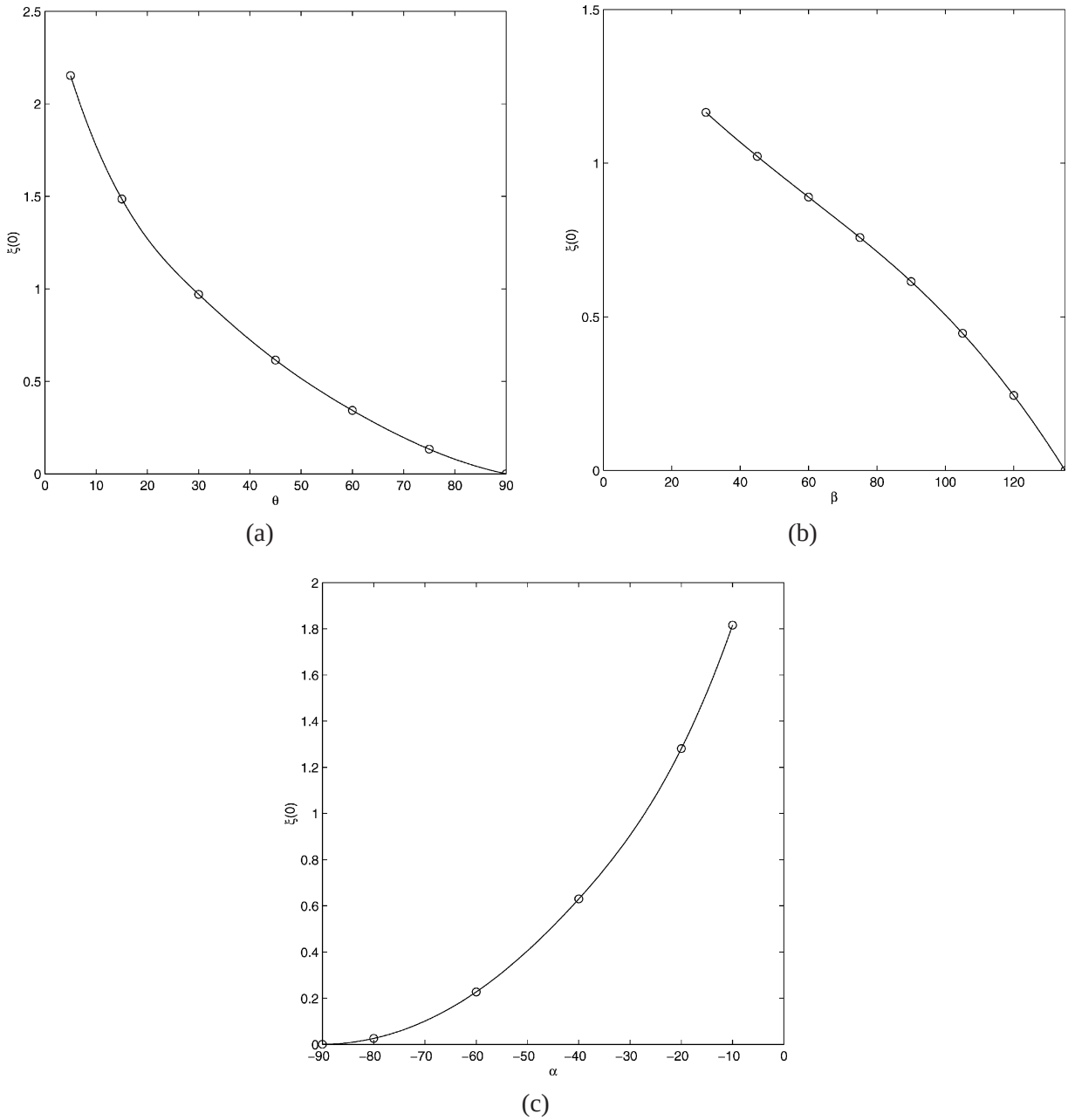

Figure 6. The wetted length OC as a function (a) of the initial angle θ, with $\alpha = 0°$, $\beta = 90°$; (b) of the contact angle β, with $\alpha = 0°$, $\theta = 45°$; (c) of the angle α, corresponding to a wedge angle $\pi + 2\alpha$, with $\theta = 0°$, $\beta = 90°$.

When *figure 2* is reflected about the y axis, it represents the wetting of a planar wall by a fluid with contact angle $\pi/2$. In that case also, the width of the wetted region and the amplitude of the capillary waves both increase as the angle θ between the wall and the fluid decreases. *Figure 6(a)* shows the half-width of the wetted region as a function of θ based upon the results shown in *figure 2*.

Figure 3 shows results for the wetting of a planar wall ($\alpha = 0$), for fixed $\theta = \pi/4$, and various values of the contact angle β. The width of the wetted region and the amplitude of the waves both increase as the contact angle β decreases. The half-width of the wetted region is shown as a function of β in *figure 6(b)*, based upon the results shown in *figure 3*. *Figure 4* shows results for $\theta = \pi/4,\ \beta = \pi/2$ and $\alpha = 0°, 15°$, and $30°$. When reflected in the y-axis, it portrays the wetting of a corner of angle $\pi - 2a$ with contact angle $\beta = \pi/2$. Both the width of the wetted region and the wave amplitude increase with α, so that they increase as the corner angle $\pi - 2\alpha$ decreases.

Figure 5 shows the results for the wetting of a solid wedge when its tip comes into contact with a fluid region at $t = 0$. This figure, when reflected about the y axis and turned upside down, yields configurations such as the one sketched in *figure 1(c)*. In this case, the width of the wetted region and the wave amplitude both increase as the angle $|\theta|$ between the fluid and the walls tends to zero. In *figure 6(c)*, based upon *figure 5*, the width of the wetted region is shown as a function of θ, and it seems to be tending to infinity as θ tends to zero.

All our results show that capillary waves are produced on the free surface of a liquid which wets a solid or merges with another body of liquid. The wave amplitude, the width of the neck of merged fluid, and the width of the wetted region of the solid all increase with decreasing angle between the neighboring surfaces of the two bodies of liquid or between the surfaces of the liquid and the solid. These same features probably occur in other cases of wetting and merging.

Padday [8] has made experimental observations under microgravity conditions of the merging of two spherical caps of liquid to form a liquid bridge, and also of the breaking of liquid bridges. He studied caps of the same liquid, and of two different liquids, with various viscosities. These experiments are not directly comparable to our calculations in which the initial surfaces have sharp corners. Nevertheless in the experiments with fluids of low viscosity, the merged surface oscillated, which corresponds to the wave motion predicted by the calculations.

The corresponding behavior for pinch-off was demonstrated in the experiment of Peregrine et al. [9]. There the water hanging from a faucet immediately after pinch-off of a drop had the shape of a short portion of a circular cone with a rounded tip. It was then pulled upward by surface tension. Capillary waves developed on its surface and its motion agreed with that of the self-similar pinch-off of Keller and Miksis [1].

Hocking [10] studied the spreading of a liquid drop on a solid by capillary action. He considered both the hypotheses of a constant contact angle and of a velocity-dependent contact angle. He concluded that the constant contact angle assumption agrees with experiment. Ablett [11] measured the contact angle and found that for an advancing liquid it increased rapidly with the velocity of the contact line and approached a constant value for large velocities. For a receding liquid the contact angle decreased to a different constant value for large velocities. These results provide some support for our wetting analysis using a constant contact angle.

On the other hand, Cox [12] analyzed theoretically the apparent or macroscopic contact angle on the assumption that the microscopic contact angle is constant. He assumed that slip occurs near the contact line and considered small values of the capillary number $Ca = \mu U/\sigma$ where U is the velocity of the contact line, μ is the coefficient of viscosity and σ is the surface tension. He found that the contact angle increased with Ca for Ca small. He also treated large Reynolds numbers, but obtained solutions only for Ca less than a certain finite value $Ca_{\max}$. Thus his results do not contradict the assumption that the contact angle tends to a constant for large values of Ca.

Suppose two bodies of fluid have surfaces which are wedge shaped with rounded tips. When they meet at their tips and merge, the flow will not be exactly self-similar. However, it is natural to expect that it will approach self-similarity as it evolves. The same behavior is to be expected when a fluid body wets a solid, both

of which are wedge shaped with rounded tips. Thus we expect the self-similar flows to be attractors for this class of flows.

Acknowledgments

J.B. Keller is partially supported by the AFOSR; P.A. Milewski and J.-M. Vanden-Broeck are partially supported by the NSF.

References

[1] Keller J.B., Miksis M., Surface tension driven flows, SIAM J. Appl. Math. 43 (1983) 268–277.
[2] Lawrie J.B., Surface tension driven flow in a wedge, Q. J. Mech. Appl. Math. 43 (1990) 251–273.
[3] Lawrie J.B., King A.C., Exact solution to a class of functional difference equations with application to moving contact line flow, Eur. J. Appl. Math. 5 (1994) 141–157.
[4] Ting L., Keller J.B., Slender jets and thin sheets with surface tension, SIAM J. Appl. Math. 50 (1990) 1533–1546.
[5] King A.C., Moving contact lines in slender fluid wedges, Q. J. Mech. Appl. Math. 44 (1991) 173–192.
[6] Popple D.F., Billingham J., King A.C., Inviscid, surface tension driven flow in fluid wedges, Proc. First UK Conference on Boundary Integral Methods, L.U.P., 1997.
[7] Miksis M.J., Vanden-Broeck J.-M., Self-similar dynamics of a viscous wedge of fluid, Applied Mathematics Technical Report No. 9710, Northwestern University, 1998.
[8] Padday J.F., The formation and beakage of liquid bridges under microgravity, Microgravity Q. 2 (1992) 239–249.
[9] Peregrine D.H., Shoker G., Symon A., The bifurcation of liquid bridges, J. Fluid Mech. 212 (1990) 25–39.
[10] Hocking L.M., Rival contact-angle models and the spreading of drops, J. Fluid Mech. 239 (1992) 671–681.
[11] Ablett R., An investigation of the angle of contact between paraffin wax and water, Philos. Mag. 46 (1923) 244–256.
[12] Cox R.G., Inertial and viscous effects on dynamic contact angles, J. Fluid Mech. 357 (1998) 249–278.